Co ultra-thin films on Pt(111) and Co-Pt alloying: a LEED, Auger and synchrotron x-ray diffraction study

1999 J. Phys.: Condens. Matter 11 8355

(http://iopscience.iop.org/0953-8984/11/43/301)

J. Phys.: Condens. Matter **11** (1999) 8355–8375. Printed in the UK PII: S0953-8984(99)04220-4

Co ultra-thin films on Pt(111) and Co–Pt alloying: a LEED, Auger and synchrotron x-ray diffraction study

R Baudoing-Savois†, P Dolle, Y Gauthier, M C Saint-Lager, M De Santis and V Jahns‡

CNRS, Laboratoire de Cristallographie, associé à l'Université J Fourier, BP 166, F-38042, Grenoble cédex 9, France

E-mail: baudoing@polycnrs-gre.fr

Received 11 May 1999, in final form 21 July 1999

Abstract. Co ultra-thin films deposited on Pt(111) are analysed in detail, using LEED, Auger spectroscopy and x-ray diffraction. The growth is quasi layer-by-layer up to about 3 ML. Co grows as islands, in incoherent epitaxy with the Pt substrate; the corresponding satellites are observed even for coverages as low as 0.12 ML. The Co in-plane parameter is very close to its own bulk value. For thicker films, deposited at room temperature, face centred cubic (fcc), twin fcc and hexagonal close packed (hcp) fractions are present.

Using x-ray diffraction, we followed in real-time the transformations of the deposited film upon annealing. The role of the Co film structure (which depends on the film thickness) is predominant. For 'thick' films ($\geqslant$6 ML) a sharp transition occurs around 670 K: below this temperature, the film is mainly hcp so that it allows little Pt incorporation, while above it turns to a very homogeneous fcc alloy of composition close to $Pt_{60}Co_{40}$. Segregation phenomena were analysed and found similar to those occurring at the surface of the corresponding bulk alloys.

1. Introduction

Metal on metal growth, particularly with a large lattice mismatch, is a subject of great interest [1]. Recent experimental investigations of alloying in ultra-thin deposits addressed important questions concerning: metastability, segregation effects, kinetics of formation of bulk alloy ordered phases and, eventually, conditions for the appearance of new phases. Simultaneously very significant progress was achieved in theoretical predictions both for deposits and for alloying within the embedded atom method [2] (EAM) or kinetic tight binding Ising model [3] (KTBIM) frames.

Apart from the intrinsic interest in the growth or in the alloying problems, obviously much research concerns the correlation of the structure and composition of ultra-thin films with their properties, mostly magnetic (including multilayer structures) or catalytic. Important changes also depend on the interface structure and on the film strain.

For instance, Leroux *et al* [4] showed that the bulk *structure and magnetism are strongly correlated for CoPt magnets with a large coercitive field in the ordered phase* ($Hc = 5000$ Oe) and a *strong anisotropy perpendicular to the 'pure' (100) planes*. Similarly, Maykov *et al* [5] found a *maximum anisotropy for the equiatomic composition, with a quadratic dependency*

† Corresponding author.
‡ Now at Science and Computing gmbh, Hagellocher Weg 71, 72070 Tübingen, Germany.

0953-8984/99/438355+21$30.00

upon the order parameter, and a *linear dependency upon the tetragonalization factor*. Band structure calculations by Kootte *et al* [6] concluded to a weak charge transfer towards Pt atoms ($<0.2\ e^-$) with a spin polarization of Pt mainly due to a very strong hybridization between the Co 3d and the Pt 5d states; again the tetragonalization was found a key parameter for this system. This was also the conclusion of Weller *et al* [7] who produced alloy films by molecular beam epitaxy (MBE) techniques and concluded that a large contribution to the magnetic anisotropy came from the 3d–5d hybridization; they even found that *the magnetic recording properties of these alloy films were better than multilayer films of similar average composition, being also easier to produce and more stable*. Finally, very recently, Beaurepaire *et al* [8] reported an *ultrafast magnetic phase transition (in the sub-picosecond range) of a* $CoPt_3$ *alloy films* about 500 nm thick in which the perpendicular magnetic anisotropy had been optimized.

The surfaces of the Co–Pt bulk alloy samples have been studied in detail, both experimentally [9] and theoretically [10]. The major effects (segregation, reconstruction, etc) are due to a subtle competition between three energy terms (elastic term due to size effects, surface tension term and chemical term with a tendency to ordering) none of which are dominating. We are interested in ultra-thin Co–Pt films, not only for magnetic properties or chemical reactions, but also to understand the forces acting during the direct growth of alloys by co-deposition. The new hexagonal Co–Pt phase, recently reported by Maret *et al* [11] might result from this subtle kinetic balance between the different surface promoted energy terms during the growth.

We report here on *in situ* and real-time studies of growth and alloying of ultra-thin Co films on Pt(111). Low-energy electron diffraction (LEED) and Auger electron spectroscopy (AES), on the one hand, and synchrotron radiation x-ray diffraction, on the other hand, were used to yield complementary results. These experimental means are briefly presented and compared in part 2. The epitaxial conditions and roughness of Co films are discussed in part 3 and alloying is then investigated in part 4. Our results are discussed with respect to previous published work.

2. Experimental details

We used two different set-ups: (i) the LEED-Auger goniometer [12] extensively used for quantitative surface crystallography analyses in our group and (ii) the ultra-high vaccuum (UHV) x-ray diffractometer [13] (so-called 'SUV') which we have installed on the French beamline dedicated to surfaces and interfaces [14] at ESRF.

The LEED goniometer is equipped with: (i) an ion pump, a titanium sublimation pump with a liquid LN_2 cooled trap and a liquid He cryopump; (ii) fully hemispherical retarding field optics, 250 mm in diameter and (iii) an electron gun, movable from normal to grazing incidence. We use a home-made TV intensified camera system to archive LEED images in real-time and extract the so-called $I(V)$ curves for most of the diffracted beams at a time. The substrate is prepared *in situ* by ion bombardment and annealing. Auger spectroscopy (retarding field mode) is usually performed with 800–1200 eV primary electrons at 20° from the grazing incidence. For a composition profile, measurements are performed as a function of the incidence angle, from normal to grazing. The sample temperature is cross-checked by thermocouple and pyrometer measurements.

The x-ray diffractometer, of the z-axis type, provides large angular ranges both for the incident and the emergent beams. It is equipped with: (i) a 400 l s^{-1} ion pump, a 180 l s^{-1} turbo pump and a titanium sublimation pump; (ii) a grazing reflection high energy electron diffraction (RHEED) gun; (iii) an Auger analyser; and (iv) several evaporation sources which can be operated during RHEED, Auger and x-ray analyses. The RHEED gun, operating at

3 keV and grazing incidence, is used for Auger analysis. The sample is also prepared *in situ* by ion bombardment and annealing with an infrared pyrometer control.

We used two Pt(111) substrate samples for this study, with small miscuts ($<0.1^\circ$ and $\sim 0.25^\circ$) and very narrow crystallite distributions ($\sim 0.015^\circ$ along the normal direction and $\sim 0.02^\circ$ in azimuth). This narrow distribution is crucial for x-ray experiments, but not so critical for LEED. The surface was prepared with classical cycles of ion bombardment (10 μA of 800 eV Ar ions, for 15 min) and annealing, at 1220 K in the first cycles and around 1070 K for routine work. The roughness was very low (~ 1 Å), as estimated from a best fit of x-ray reflectivity measurements.

Clean surfaces were routinely obtained, as controlled with Auger spectroscopy, apart from a very small residual carbon contamination (approximately very few per cent of a monolayer); no other contaminants were detected.

Co was deposited from an EFM4 Omicron source, with a 4N5 Co rod. The integrated flux monitor is accurate, and computer controlled to obtain reproducible films. Our deposit rate was typically one Co monolayer (ML) in 4 min. The thickness was calibrated either from intensity oscillations of the specular reflexion (RHEED or x-ray experiments), or from the breaks in the ratio of the Auger Pt and Co lines versus time; good consistency was obtained. The base pressure was below 5×10^{-10} mbar even during evaporation.

3. Complementarity of LEED and 'grazing' x-ray diffraction

LEED and surface x-ray diffraction involve quite different interactions of electrons and photons with surfaces. We show in this paper how complementary they are to analyse metal film growth and alloying with a metallic substrate.

A first major difference is that LEED offers an instantaneous two-dimensional (2D) projection of a spherical section of the reciprocal space, while lengthy scans need be performed with x-rays. In addition, LEED is always available, while very limitated time is available for synchrotron x-ray experiments.

More subtle consequences occur from the huge difference in their interaction with matter:

- LEED is 'always' in a situation of strong multiple scattering and weak penetration, anywhere in the reciprocal space. On the contrary, for x-rays only regions far from the three-dimensional (3D) Bragg bulk peaks are significantly sensitive to surface parameters.
- structural parameters can be easily separated in x-ray diffraction, according to the kinematical diffraction theory: as recently discussed by Vlieg *et al* [15], the sensitivity to a given geometrical parameter depends on its projection on the scattering vector. In surface x-ray diffraction experiments, scattering vectors often have a dominant projection parallel to the surface and hence are most sensitive to displacements parallel to it. However this kinematic type of argument does not apply to LEED, where strong multiple scattering completely mixes the sensitivity to parallel and normal components of the geometrical parameters [16].
- the 'reference structure' is also quite different in both experiments. In standard LEED, the 'visible substrate' is typically 10–20 layers thick at most, while it is much more in x-ray studies, even close to grazing incidences. This is a concern in quantitative LEED studies of ultra-thin films since their lattice constant may change by strain effects or simply, if it is a compound, by a composition to be determined simultaneously with a lattice constant. We have recently reported on this sensitivity of LEED to the 'bulk' parameters of a PtCo alloy [17]!
- stacking faults or the presence of different crystallographic phases in a film can easily

be detected by x-rays, as shown below, and this is a key contribution. Actually, stacking faults close to the surface also perturb LEED intensities very significantly and could even be used as 'fingerprints', as recently suggested by Ascolani *et al* [18].

- most remarkably, it has recently been shown that even if no superstructure spots were observed in LEED, intensities are modified by local chemical ordering, essentially because of strong multiple scattering effects [19] (see also the review by Gauthier [9]).
- x-rays can very efficiently supply:
  * accurate parameter measurements relative to the substrate (always visible),
  * film thickness (if the interface roughness is not too important),
  * various compound phases present in the film,
  * real-time analysis of the annealing processes, to quite high temperatures,
  * long range and local structural informations with chemical selectivity (our diffractometer allows for diffraction and surface extended x-ray absorption fine structure (SEXAFS) experiments in the same run).

However, the price to pay for quantitative information is much better crystal quality is required for x-ray experiments than for LEED (crystallites can ruin quantitative x-ray analysis while one often finds a 'good' area on the surface for reliable LEED measurements).

We close this section with the presentation of the reciprocal space coordinates suited for our analysis of the Pt(111) surface with both techniques (figure 1). The reciprocal space is based on two surface vectors a^* and b^*, which define a 2D hexagonal lattice (indices H and K), and on rods (index L) perpendicular to the surface at each 2D lattice node. Different paths will be followed during x-ray experiments: H- or K-scans (parallel to the surface along the (10) or

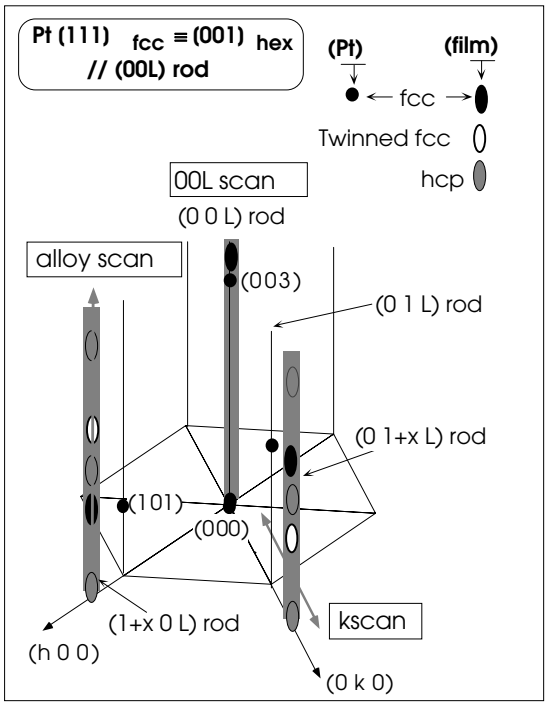

Figure 1. Pt(111) reciprocal space; description adapted to the surface experiments and scans used in the x-ray analysis.

(01) directions) and L-scans (perpendicular to the surface). In the following H, K and L are normalized to the Pt lattice parameters.

4. Growth of Co films on Pt(111)

The lattice mismatch between Co and Pt is large (∼10%) and the question of a pseudomorphic growth for the first few Co layers is actually quite controversial! We studied Co deposits on a Pt(111) substrate at room temperature, for increasing thicknesses, from 0.1 to 10 ML, with LEED–Auger techniques [20] and with x-ray diffraction [21]. A synthesis of our results is presented here, and compared to those available in the literature.

4.1. Present results

4.1.1. LEED and Auger analysis. We first followed the LEED patterns obtained for cumulative Co doses, from very small amounts up to 10 ML. We calibrated the coverage from the ratio of the high energy Co_{775} and Pt_{237} Auger peaks as a function of deposition time (figure 2); we obtained clear breaks about 4 min apart, indicating a quasi layer-by-layer growth up to about three layers.

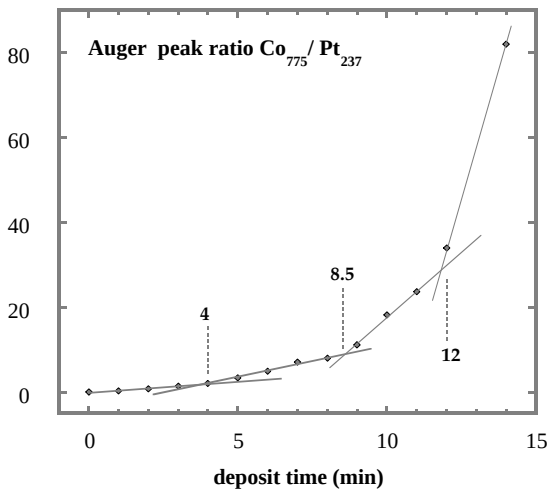

Figure 2. Coverage calibration from Auger measurements: about 1 ML is deposited in about 4 min.

Normal incidence patterns in the sub-monolayer range are presented in figure 3; only one quadrant is shown. In the lower right corner, the electron gun is hiding the specular spot. Small hexagons of satellites are present around the Pt substrate spots: they appear already at 0.12 ML and become very well defined around 0.2 ML. They mimic the Pt reciprocal lattice (same orientation but only about 1/10th in length) and only the first-order satellites are visible at low coverage. Note also that they are very sharp, indicating Co islands of significant size even for quite low coverages. This size is comparable to the transfer width of our LEED goniometer, which is about 150–200 Å; the satellites slightly broaden for cumulative deposits, as shown in figure 4 for 1 ML and 4 ML films. The satellites are still present for 5 ML, they are quite narrow although with faint intensity.

At low coverages the symmetry of the pattern is clearly three-fold, but the intensity of a star of satellites is rather six-fold around a Pt spot. As the thickness increases, the pattern

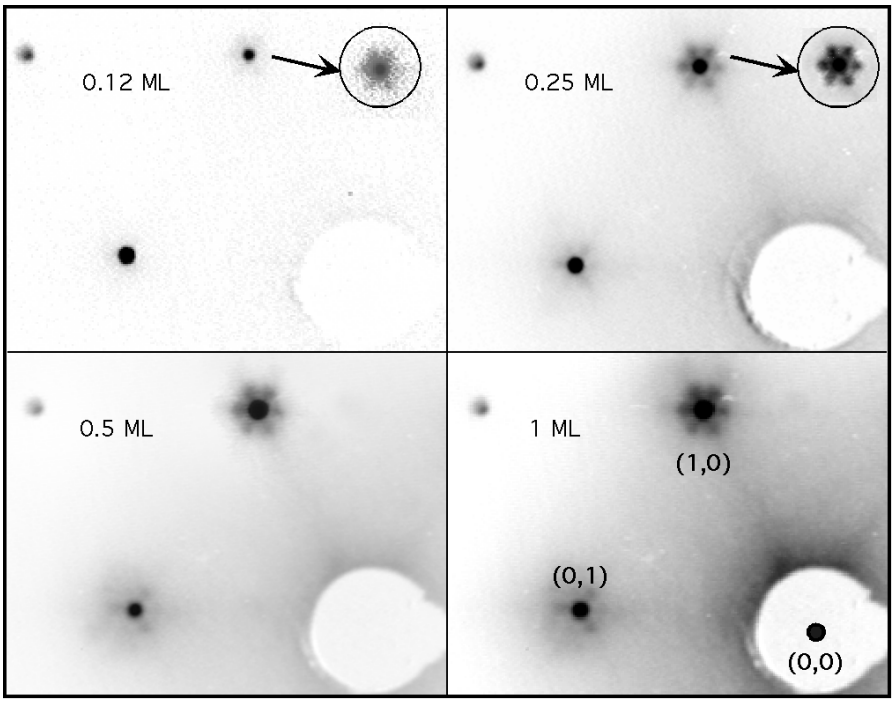

Figure 3. LEED patterns (one quadrant only) showing satellites for sub-monolayer Co cumulative deposits.

becomes more complex, with higher-order satellites particularly well visible from 1 to 4 ML (figure 4). Around 2–3 ML the respective (10) and (01) spots of Pt and Co have comparable intensity: below, Pt spots dominate at the centre of the satellite star, while above 3 ML, Co spots become more and more intense and the satellites organize around them. Above 5 ML, the Pt substrate spots are no longer visible and the three-fold symmetry transforms into a pseudo six-fold symmetry.

While the sequence of observed patterns remains similar, the spots are much sharper when the film is grown in one run instead of cumulative deposition (figure 4). In the following we only report on direct deposits.

One can estimate the in-plane parameter of the Co film by comparing the respective LEED patterns from the substrate and from the deposit. Within our accuracy ($< \pm 1.5\%$) we estimated the Co film to be relaxed to its bulk parameter for the 4 and 10 ML films and possibly slightly strained for the 1 ML film; but from the very beginning, even for very low coverages ($\sim$0.12 ML) the parameter is almost that of bulk Co.

4.1.2. Synchrotron diffraction analysis. We then performed several campaigns [22] of x-ray measurements for different deposits using H- and K-scans to determine the in-plane reciprocal lattice constant and L-scans to analyse the film stacking and thickness.

The film roughness was much less pronounced than that reported by Ferrer *et al* [23], according to the specular reflectivity versus deposition time (figure 5). Up to about three layers, the growth is close to layer-by-layer, with relatively little roughness. Above 3 ML, our films become rougher but we still observe good LEED patterns.

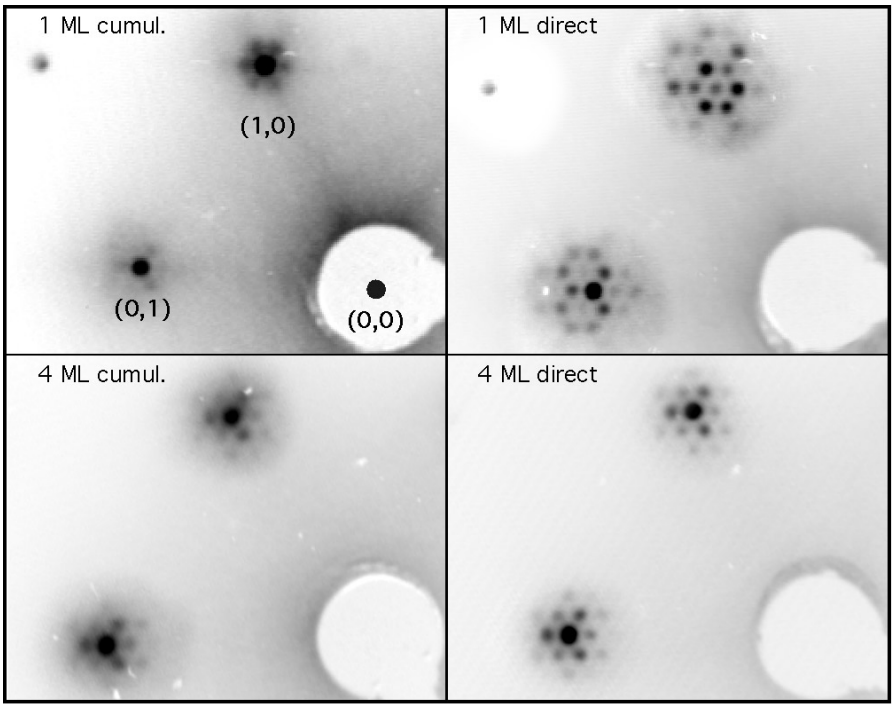

Figure 4. LEED patterns are of much better quality for direct deposits than for cumulative deposition.

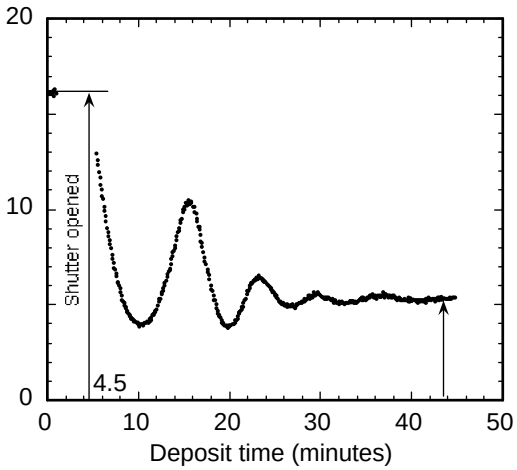

Figure 5. Variation of the specular reflectivity against deposition time.

The specular intensity distribution (so-called 'L-scan') along the (0 0 L) rod after the growth of 3, 6 and 10 ML, is presented in figure 6. L-scans are shown for each film at room temperature and after gentle annealing at 500 K. The oscillations (Kiessig fringes) are due to interferences between the waves reflected at both interfaces of the film, which allows one to count the number of deposited layers. After annealing, their 'contrast' was significantly

improved, revealing more abrupt interfaces. This effect is more pronounced for the 10 ML film: the 3D islands of the room-temperature film are smoothed leading to a flatter surface. The 3 ML film, resulting from a quasi layer-by-layer growth, was already smooth enough at room temperature and the contrast was already large.

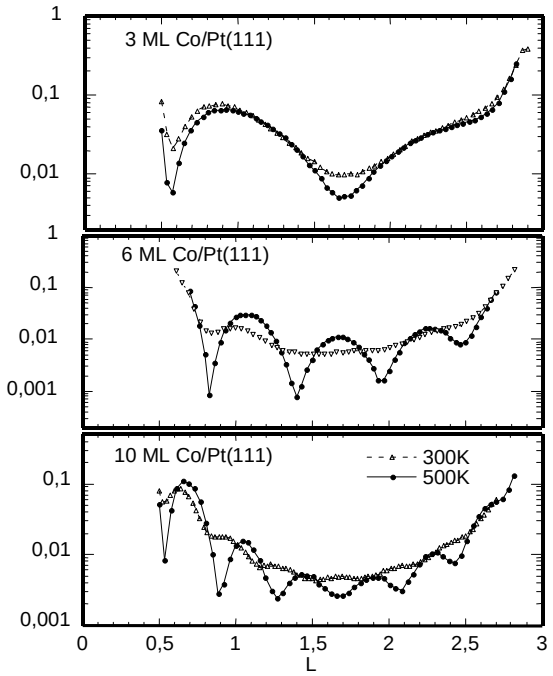

Figure 6. X-ray specular intensity distribution along the (0 0 L) rod after the growth of 3, 6 and 10 ML films, at room temperature and after annealing at 500 K.

We then analysed the intensity distribution of the (1.1 0 L) rod of the Co film. After substraction of the thermal diffuse intensity due to the Pt substrate, we identified clear contributions from coherent face centred cubic (fcc), twinned fcc and hexagonal close packed (hcp) phases, which are simultaneously present in the room-temperature as-deposited films. After annealing at 500 K, the hcp component dominated while the twinned fcc fraction almost vanished.

4.2. Summary and comparison with previously published works

The situation is different according to the film thickness.

4.2.1. 0.12 to ~ 2 *ML Co films.* We do observe well defined and narrow satellites in the LEED pattern already for very low coverages, we thus disagree:

- with McGee *et al* [24], Atrei *et al* [25] and Thiele *et al* [26], who report a (1×1) LEED pattern and conclude to a pseudomorphic first Co layer;
- with the interpretation of scanning tunnelling microscopy (STM) images of Grüter and Dürig [27], who draw the same conclusion;
- with Tsay and Shern [28], who report only fuzzy background in (1×1) LEED patterns below 0.8 ML while, above, they report the same satellites as we see.

On the other hand, our results would explain why Ferrer *et al* [23] claimed a quadratic dependency of the satellite intensity at $k_{\parallel} = (0, 1.097)$ as a function of deposit time, and concluded to Co layers almost fully relaxed to their bulk parameter from the very beginning. Moreover, the widths of our *satellites* are comparable to those of the substrate spots. This is consistent with the STM images of Grüter and Dürig [27] which show a large mean diameter (73 Å) of the Co islands, even for 0.2 and 0.57 ML coverages.

4.2.2. 2 to ∼10 *ML Co films.* For larger thicknesses, our results are closer to some results of the above cited authors, although with some differences.

- We do observe *nice satellites* up to 5 ML but none at 10 ML (we made no observation in between). Practically all authors find satellites in the range 2–4 ML. Tsay and Shern [28] report satellites up to 7 ML, probably the upper limit of their existence.
- The growth is quasi layer-by-layer up to about 3 ML: this is a more or less common conclusion to STM (Grüter and Dürig [27]), core level shifts (Thiele *et al* [29]) and our LEED and x-ray analyses. From STM images Grüter and Dürig report the first and second layer percolations to occur around 0.8 and 1.8 ML, but above 3 ML they show a 3D island growth (pyramids). At the same time, the roughness was such that as many as four to seven levels were present simultaneously. Our films seem, however, to contain fewer faults and be smoother than in some reported works: our specular intensity oscillations (figure 5) are much more pronounced than in Ferrer's work [23].
  We identify fcc, twin fcc and hcp phases in our 6 and 10 ML thick films; gentle annealing (∼420–550 K) makes hcp the dominant phase. Some hcp phase was also found present by Thiele *et al* [29] from EXAFS analysis of Co films: above 2 ML, they concluded to the same first-neighbour distances as in bulk Co, and between 4 to 10 ML they described 'the films as an hcp structure very similar to bulk Co.' Finally, Grüter and Dürig [27] also concluded to a stacking, mainly hcp, from the orientation of the triangular shaped pyramids of the film. From our present work the room-temperature films are a mixture of phases rather than a simple hcp phase.
- The lateral size of the Co coherent domains is already significant at room temperature. This is clear from the width of the LEED satellites (comparable with the substrate spots). A quantitative estimation of about 200 Å is obtained from the width of the satellites at $k = 1.1$ in the K-scans. Actually a similar value is obtained for the Co film deposited at room temperature and for the film annealed at 470 K for a few minutes. This is in rough agreement with the results of Ferrer *et al* [23] who, however, indicated such a value only for the annealed film.
- Tsay and Shern reported [28] a p(2 × 2) superstructure in the temperature range 140–600 K and for coverages above 4.5 ML. They interpreted this as due to steps. We did not observe this, but our samples had a very low miscut and narrow crystallite distribution.

5. Surface alloying

The surface structures of bulk PtCo alloys have been investigated by quantitative LEED analyses (see [9, 17] for example), and segregation effects have been shown to depend on atomic size, surface tension and ordering energy terms. However, little is known on the alloying of a metal A deposited on a metal B which exhibit different bulk structures. Several Co films are discussed below, showing different behaviours depending on the initial thickness.

The Pt–Co system exhibits a simple bulk phase diagram (figure 7) according to the recent contribution of Leroux *et al* [4]. The alloy has a $L1_2$ structure around $PtCo_3$ and Pt_3Co and

$L1_0$ around PtCo. Noteworthy is the limited amount of Pt that can be incorporated into hcp Co before it turns to fcc [30]. The bulk parameters of substitutional Pt_xCo_{1-x} alloys in the whole range of composition measured by Dahmani [31], is also indicated.

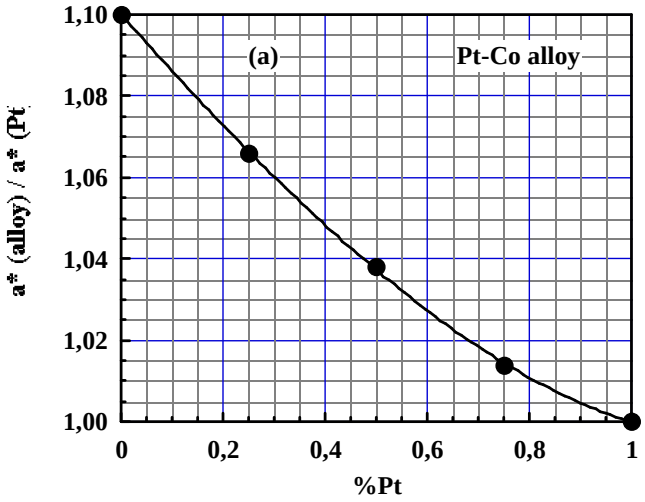

(a)

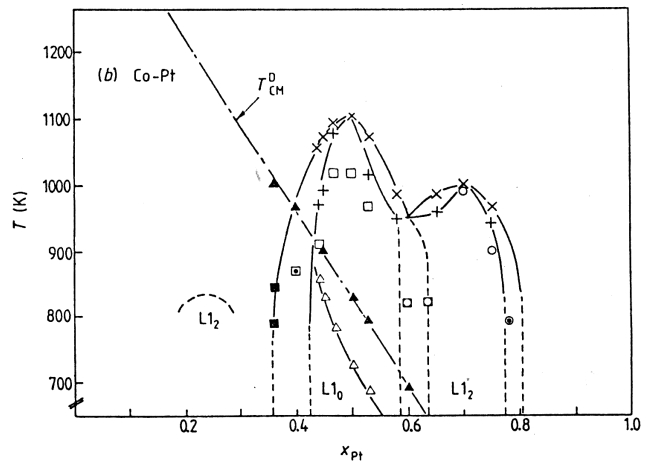

(b)

Figure 7. Pt–Co alloy. (a) Relative value of the alloy lattice parameter determined by Dahmani [31] in reciprocal units, normalized to the Pt value. (b) Alloy phase diagram according to Leroux *et al* [4].

5.1. Present results

We consider Co films from 1 to 10 ML, to span situations from an adsorbed layer to a system dominated by surface effects and finally to a film where bulk behaviour might dominate. We used complementary investigations (LEED, AES and x-ray synchrotron techniques) with particular interest in:

(i) the real-time evolution upon annealing (structural and compositional changes),

(ii) the metastable alloys obtained for different annealing (thickness, components present in the film, roughness and segregation effects), and
(iii) the film–substrate interface.

5.1.1. LEED and Auger analysis.

Surface structure. Annealing the 1 ML film at about 600 K leads to a metastable state: the LEED pattern shows weak triplets of satellites, centred on the substrate spots, the satellite along the (01) direction is positioned at $k = 1.035$.

After annealing the 4–10 ML films, typically 30 min, we identify two different alloy states around 640 K (LT) and 700 K (HT) with respectively six- and three-fold symmetry patterns. The spot position also changes upon alloying, pointing to slight Pt enrichment for the LT alloy and a richer Pt composition for the HT alloy. The film compositions were estimated from the known bulk alloy parameters (figure 7).

This is illustrated for a 4 ML film (figure 8): the satellites disappeared leaving only shifted single spots. For the LT alloy the satellites are slightly broader than for the Co film, and correspond to about $Pt_{15}Co_{85}$. For the HT alloy the shape is clearly triangular, in fact a triplet of unresolved satellites around a central spot which corresponds to about $Pt_{55}Co_{45}$. Such triangular shapes were however not observed for the HT annealed 10 ML film.

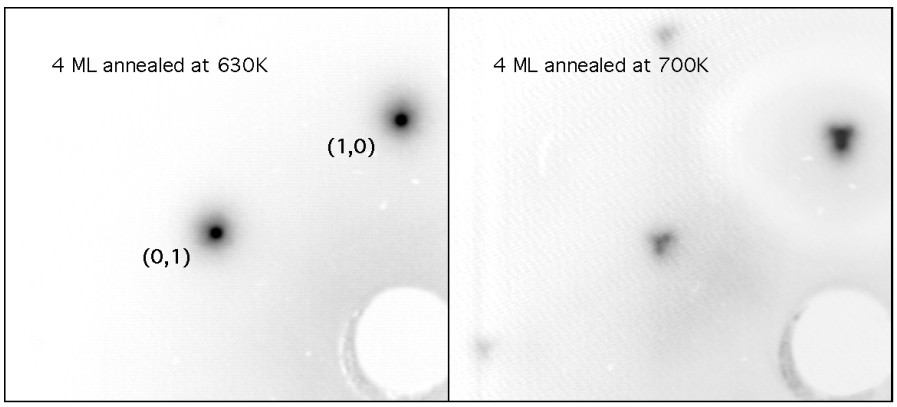

Figure 8. LEED patterns for the alloys obtained by annealing 4 ML Co at 630 K (LT) or 700 K (HT).

The apparent six-fold symmetry (LT) could either be due to a dominant hcp component or/and to fcc and twin fcc domains of comparable weight in the film. Although the answer could come from quantitative LEED analysis, we show below that x-ray diffraction provides a 'fingerprint' which solves the question.

The symmetry clearly turned to three-fold for the HT alloy, indicating a major fcc-like component, coherent with the substrate. Partial ordering was also observed in this case with faint p(2×2) superstructure spots. Chemical ordering is not surprising: local order was observed, for instance, in the top layer of $Pt_xNi_{1-x}(111)$ and $Pt_{25}Co_{75}(111)$ bulk alloys. STM images showed small areas of (1×2) reconstruction with alternating Co and Pt portion of rows [32] and interestingly LEED calculations also clearly indicate ordering, although no superstructure spots were present ([9, 19]).

Segregation effect. Auger analysis was performed for a 4 ML deposit on both alloy states (LT and HT) using 800 eV primary electrons. The modification of the surface region composition

was followed via the ratio of the Pt_{64} and Co_{53} Auger peak amplitudes, plotted against the incidence angle (figure 9).

- The measurements confirm the compositions indicated from the LEED spot positions for the LT alloy (slightly Pt enriched) and HT alloy (medium Pt composition): comparison with bulk alloys previously studied [33] (also shown on figure 9) suggests about $Pt_{25}Co_{75}$ and $Pt_{50}Co_{50}$ for the LT and HT alloys.
- At grazing incidence ($\theta \geqslant 70^\circ$) the ratio increases, a direct proof of Pt segregation in the top layer. If segregation follows the trends (figure 10) which we have determined for the (111) surfaces of bulk PtNi and PtCo alloys ([33], see also [17] for $Pt_{35}Co_{65}(110)$) we expect Pt compositions in the top and second layers to be $C_1 \sim 85 \pm 10\%$ and $C_2 = 15 \pm 15\%$ for a 'bulk' composition of ∼50%.

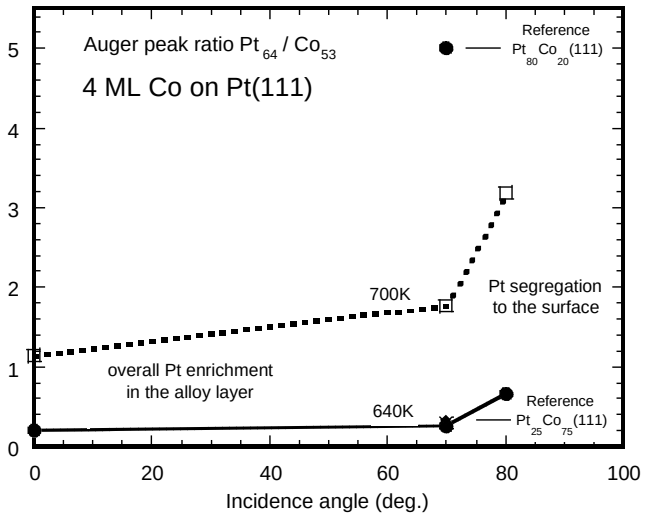

Figure 9. Variation of the ratio of Pt/Co Auger lines as a function of the incidence angle ($\theta = 0$ corresponds to normal incidence).

A quantitative LEED $I(V)$ analysis was started for a thick 10 ML film, annealed at 700 K, to guarantee a sufficiently homogeneous and thick alloy 'substrate' below the topmost segregated layers. Preliminary results indicate the following compositions: alloy film $C_{bulk} \sim 55$ at% Pt and topmost layers $C_1 \sim 85\%$ and $C_2 \sim 0\%$.

5.1.2. Synchrotron radiation analysis

Structure analysis of the alloy obtained by annealing a 1 ML Co deposit. We performed a full x-ray structure analysis of the surface metastable alloy obtained by annealing a 1 ML Co deposit at about 600 K for typically 15 min. The superstructure satellites observed by LEED were not measurable by x-ray diffraction, due to a lower scattering cross-section. However, the intensity distribution of the substrate rods were significantly modified.

The x-ray structure analysis was thus performed using 220 independent data sampled from the (0 0) (1 0) (0 1) (1 1) (1 2) and (3 0) rods, we optimized the compositions for the three outermost layers and their interlayer distances (table 1). The oscillating composition profile, $C_1 \sim 80$ at% Pt and $C_2 \sim 20\%$, is fully dominated by segregation.

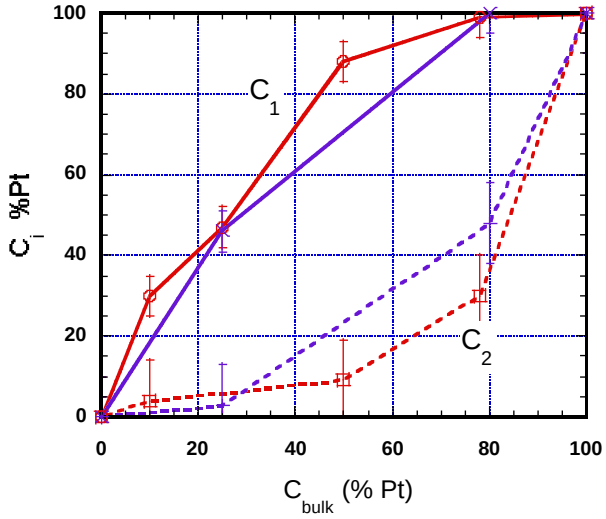

Figure 10. Segregation at the surfaces of bulk alloys: general trends for PtNi and PtCo (111) for the top (C_1) and second (C_2) layer concentrations as a function of the bulk alloy composition (C_{bulk}).

Table 1. Surface structure for the metastable alloy obtained by annealing 1 ML Co at about 600 K.

	d_{12} (Å)	d_{23} (Å)	C_1 (at% Pt)	C_2 (at% Pt)	C_3 (at% Pt)
This study (x-ray)	2.11	2.01	80	20	90
Atrei *et al* [25] (LEED*)	2.16	2.01	80	20	

Real time analysis of alloying. X-ray diffraction was then used to follow the real-time evolution of 3, 6 and 10 ML thick films. As for the RT Co films, we used: (i) K- or H-scans running across the substrate and alloy rods; and (ii) L-scans along substrate and alloy rods, a particular case being the specular reflection rod ('0 0 L') which mixes both informations.

Upon annealing, the thinner (3 ML) and thicker (10 ML) films differ greatly. This is illustrated (figure 11) via a map of K-scans as a function of temperature which is raised linearly [34] between 470 K and 730 K in 20 K steps, each one being 20 min long. The main results, fully discussed elsewhere [35], are summarized here.

- Whatever the thickness, annealing up to 470 K induces no interdiffusion and no change in the satellite position. It rather efficiently smoothes the film, as shown by the enhanced Kiessig fringes in the specular rod (figure 6). We note that the '10 ML' deposit is in fact rather 9 ML thick, once it is smoothed (figure 12).
- Above 470 K, the story depends on the initial film thickness (figure 11): the film rod position changes smoothly with temperature (from $k = 1.1$ to 1.04) for the 3 ML film whereas, for the 10 ML film, it is 'locked' (to $k = 1.1$) up to ∼670 K where a transition to a well defined alloy occurs, with an in-plane lattice parameter corresponding to about $k = 1.032$. We point out, however, that the final HT alloy is similar for both thicknesses ($\sim Pt_{60}Co_{40} \pm 5\%$).
- Simultaneously, the *overall thickness of the film* (derived from the (0 0 L) oscillations), *gradually increases for the thin film while there is a fast increase above 670 K for the thick film (figure 12).*

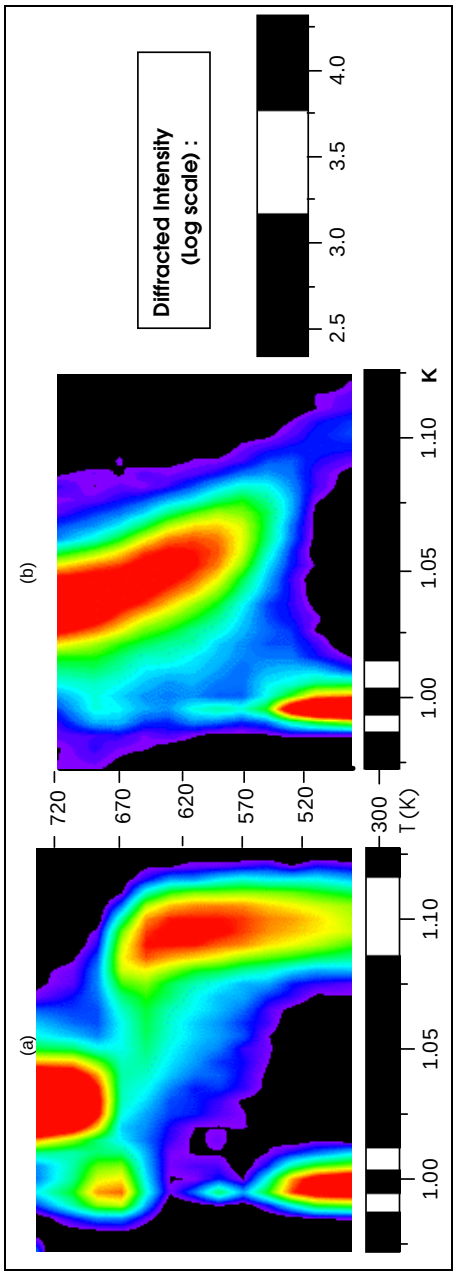

Figure 11. Mapping of the diffracted intensity in the K space against temperature, for (a) 10 ML and (b) 3 ML films.

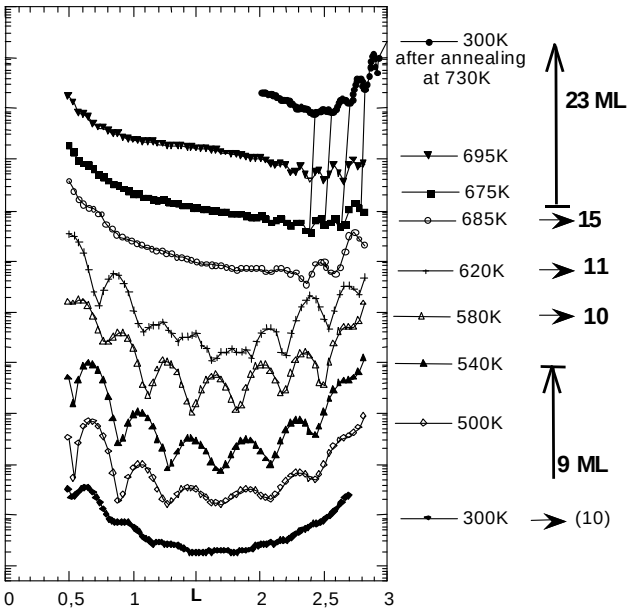

Figure 12. Kiessig fringes along the specular rod (0 0 L). These oscillations are directly related to the film thickness and give a feeling of the interface roughness.

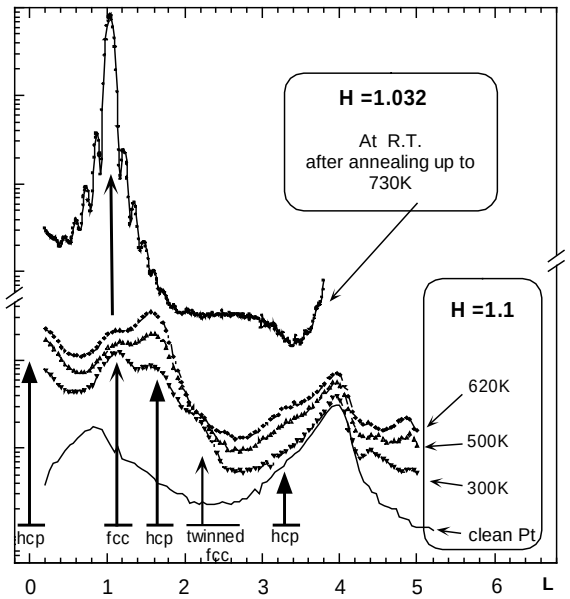

Figure 13. Intensity distribution along the non-specular (H 0 L) alloy rod for the 10 ML film, as a function of temperature.

- Finally, the non-specular rod of the 10 ML film (figure 13) at room temperature exhibits components with maximum intensity around L = 1.1 and 4.4 (fcc stacking), L = 2.2 (twinned fcc stacking) and L = 1.65 and 4.95 (hcp stacking). Above 470 K these

components start to change: the twinned fcc fraction decreases while the hcp one increases up to 670 K. At this temperature, there is a transition (the rod shifts from $k = 1.1$ to $k = 1.032$) and *the stacking suddenly changes from mainly hcp to only fcc* (coherent with the substrate stacking). The top curve in figure 13, was taken after cooling to room temperature: the alloy rod, at $k = 1.032$, showed well defined Kiessig fringes proving well defined interfaces. Moreover *the thickness of this alloy component was very close to the overall thickness of the film* (23 ML) deduced from the (0 0 L) intensity oscillations (figure 12). This is a proof that, *at 730 K, the alloy is very homogeneous extending from vacuum down to a sharp Pt interface*.

Simultaneously, the (0 0 L) rod intensity is strongly modified: a very broad weak maximum appears around L = 1.5. Semi quantitative simulations point to *segregation* concerning the two outermost layers (a Pt rich top layer and a Co rich second layer), in very good agreement with the preliminary quantitative LEED results.

All our experiments point to a smooth alloying phenomenon for the thin 3 ML deposit, but to a rather abrupt transition for the thick 10 ML film. This transition, which looks like the martensitic transition of bulk cobalt, does not exist below a critical thickness (hcp or fcc stacking does not make much sense in the 3 ML case while it is meaningful for the 10 ML case).

We find consistent pictures between the LEED, Auger and x-ray results. For the '10 ML' deposit, annealing at 720 K yields an homogeneous alloy 23 layers thick, corresponding to an average composition of $[(23 - 9)/23]100\% = 61\%$. The LEED and Auger studies presented above, conclude to a 'bulk' composition of $Pt_{55}Co_{45}$. As regards the segregation, x-rays do confirm the Pt concentration oscillations found by quantitative LEED analysis (see section 5.1.1).

Pt–Co interface. From the Kiessig fringes in the (0 0 L) rod, we deduce the number of layers ΔML which, upon annealing, add up to the 3, 6 and 10 ML Co films (figure 14).

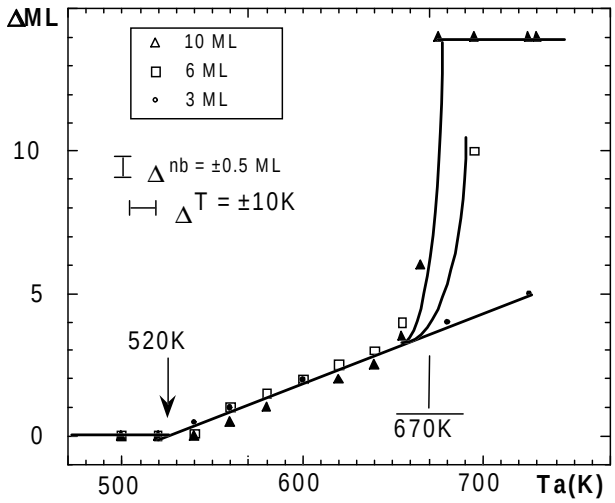

Figure 14. Number of layers adding up to the original Co film upon annealing.

Up to about 640 K, ΔML is independent of the initial thickness: this suggests that alloying is controlled by a local equilibrium process at the interface, concerning only one or two layers

on each side [36]. A more detailed discussion will be presented elsewhere.

Ordering. Above 670 K, superstructure rods appear in the 3, 6 or 10 ML films, simultaneously with the fcc alloy phase. Their width points to a rather long-range chemical ordering and their 2D coordinates agrees with our observation of a faint p(2×2) LEED superstructure for the HT alloy obtained from the 10 ML Co film. Anomalous x-ray scattering measurements at the Co K and Pt L_{III} edges, allowed us to determine the structure factor of the superstructure reflections and to prove the existence of chemical order. This order is compatible either with a $L1_2$ structure or with three domains of the $L1_0$ structure; the average composition $Pt_{60}Co_{40}$ does not help since it is close to the boundary between both bulk phases. We only emphasize here that it could even be a mixture, as recently reported by Ristau *et al* [37], who pointed out the role of $L1_0$ nano-precipitates in fcc PtCo thin films to yield large magnetic anisotropies and large coercitivities. A more complete description and discussion is given elsewhere [38].

5.2. Discussion and comparison with previously published work

5.2.1. Evolution of the film upon annealing. The overall evolution of the alloying process, depends on the film thickness.

1 ML Co film. The metastable annealed film at about 600 K can be understood according to the comparison between the LEED and x-ray diffraction results.

Weak triplets of superstructure satellites, were observed by LEED around the substrate spots, but were not measurable by x-ray diffraction. At the same time, significant modifications of the x-ray intensity distribution along the substrate rods are found. This strongly suggests that most atoms in the superficial film are in registry with the substrate and that the LEED satellites may come from periodic defects. Indeed the two outermost layers have a very different Pt concentration ($C_1 \sim 80\%$ and $C_2 \sim 20\%$, table 1) which would correspond to a 7% lattice mismatch for homogeneous alloys (figure 7): this can generate strains easily relaxed by means of defects.

At this stage, we also point out that the position of the LEED satellites at $k = 1.035$, would correspond (figure 7) to the parameter of an $Pt_{50}Co_{50}$ homogeneous alloy film. This composition turns out to be equal to the average of the two outermost layers. Whether this is only a coincidence or it has a real meaning via a subtle equilibrium between segregation effects and elastic and chemical enthalpy terms, we cannot tell.

These findings on annealed 1 ML Co films are consistent with previous results. Tsay and Shern [28] only report a fuzzy diffuse intensity around the Pt spots. Atrei *et al* [25] report only a (1×1) pattern without satellites, but their LEED $I(V)$ analysis yields optimum structural parameters in very close agreement with those presented here (table 1).

'Thin' Co films. For thin Co films that are about three to four layers thick the alloying process proceeds continuously. The film structure remains essentially fcc up to about 470 K, where it becomes smoother and contains fewer faults, but where no significant interdiffusion has started yet. Above 470 K, the composition changes smoothly from pure Co to about $Pt_{60}Co_{40}$ around 720 K.

Qualitatively we only partially agree with Thiele *et al* [29] who reported a $Pt_{25}Co_{75}$ alloy after annealing 4 ML Co at 670 K for about 20 min. Actually we showed that both the Co thickness and the annealing conditions control the alloy composition:

- for 3 ML Co (analysed with x-rays) we found about $Pt_{40}Co_{60}$ (LT) at 640 K, which rises to about $Pt_{55}Co_{45}$ at 690 K (see figures 11 and 14).
- for 4 ML Co (analysed with LEED and AES) we found about $Pt_{15–25}Co_{85–75}$ (LT) at 640 K, which rises to about $Pt_{50–55}Co_{50–45}$ at 690 K (see figures 9 and 14). The composition which we obtained after annealing at 640 K for 20 min (figure 9) is close to the result of Thiele *et al*, but there is some deviation from our quite general behaviour shown in figure 14. We thus suspect that the annealing time was too short and/or a possible difference in the actual annealing temperature performed in different UHV set-up.

The results of Ferrer *et al* [23] for a 4 ML Co film annealed at 600 K for 10 min, seem to correspond to a transient state rather than to a well defined metastable state. This is probably why several components co-exist in their surface alloy.

'Thick' Co films. For thick Co films that are about nine to ten layers thick the alloying process proceeds discontinuously. The film (a mixture of fcc, twin fcc and hcp components at room temperature) changes to a dominant hcp phase to about 470 K, where it becomes smoother and contains fewer faults with practically no interdiffusion. Above 470 K, the composition changes little up to 640 K, except in a very limited region close to the interface. Around 670 K the film structure changes abruptly (on a minute time scale) from mainly hcp to an fcc-like $Pt_{60}Co_{40}$ alloy that is homogeneous over the whole film thickness. *This alloy is metastable against annealing up to 730 K. Simultaneously with this lattice transformation (similar to the bulk Co martensitic transformation) order starts to develop.*

The smoothing found for annealing temperatures slightly below 470 K is consistent with the growth of Co islands and the disappearance of the small on-top clusters visible on the STM images of Grüter and Dürig [27].

The results of Ferrer *et al* [23] for an 8 ML Co film annealed at 600 K for a few minutes, are interesting but very different from ours owing to the transient nature of their observation. The topmost $Pt_{10}Co_{90}$ component was no longer observed, the deeper components $Pt_{25}Co_{75}$ and $Pt_{45}Co_{55}$ appeared only for a short time and quickly decreased to leave a dominant $Pt_{75}Co_{25}$ component, which we did not observe in our case! They did not report on ordering.

5.2.2. Existence of a high temperature metastable alloy, independent of the deposit thickness.

- *Whatever the Co thickness in the range 3–10 ML, the same metastable alloy is obtained for annealing temperatures* $\geqslant$*690 K. It corresponds to a composition about* $Pt_{60}Co_{40}$*, in which order develops, compatible either with an* $L1_2$ *phase or a combination of 3* $L1_0$ *domains*. The 1 ML film actually requires a lower temperature (600 K) to produce this composition. Thiele *et al* [39], from EXAFS analysis also conclude to an homogeneous $Pt_{60}Co_{40}$, alloy by annealing 4 ML Co at 700 K for 20 min.
- For films $\geqslant$6 ML thick, *two different alloy states are obtained upon annealing around 640 K (about* $Pt_{10}Co_{90}$*) or around 720 K (about* $Pt_{60}Co_{40}$*).* The apparent six-fold pattern symmetry for the LT alloy is explained by a mixture of hcp, fcc and twin-fcc domains; we have shown that the hcp component was much favoured by annealing (in agreement with Ferrer's results [23]), which in turn does not allow for much Pt incorporation. The HT alloy, on the opposite, is fcc and exhibits a clear three-fold pattern symmetry. Such LEED observations were not reported by Tsay and Shern [28], although they are straightforward.
- Auger spectroscopy operated at grazing incidence revealed significant Pt surface enrichment for both alloy states due to segregation effects, similar to those occurring at surfaces of bulk alloys of comparable compositions [33]. These findings are consistent with the results of Thiele *et al* [26].

6. Summary

We report on extensive studies of Cobalt ultra-thin films (between 0.12 and 10 ML) deposited on Pt(111). We used a combination of LEED, Auger spectroscopy and *in situ* x-ray diffraction, and we discuss our results with respect to previous works.

From the very beginning (i.e. 0.12 ML) of the Co growth at room temperature on Pt(111) we observed well defined and narrow satellites around the Pt LEED spots, at variance with most of the previous works. For thicker layers the growth is found quasi layer-by-layer up to 3 ML, and much rougher up to 10 ML. The in-plane lattice parameter relaxes practically to the bulk Co value from the beginning. The stacking is a mixture of fcc, twinned fcc and hcp phases.

Upon annealing, the film becomes much smoother around 470 K, while significant interdiffusion at the substrate interface only begins around 500 K. Increasing the temperature (we used a linear heating program) leads to alloying in a way which strongly depends on the initial thickness of the Co film:

- In the case of 1 ML Co, annealing at 600 K leads to a surface alloy with a reversed composition profile: the top and second layers are respectively Pt and Co very rich. Most of the atoms of this surface alloy appear to be in registry with the Pt substrate, according to the quantitative analyses of our x-ray data and to the LEED analysis published by Atrei *et al* [25]. Our LEED images suggest that periodic defects are also present.
- For thin Co films (3–4 ML) the alloying proceeds continuously while the temperature is raised; the surface alloy becomes richer in Pt, up to a metastable composition of about $Pt_{55}Co_{45}$, at around 740 K.
- For a thick film (9–10 ML) the behaviour is very different: little Pt ($\leqslant$15%) is incorporated in the film which is mainly hcp up to a temperature of around 670 K. At this point a rapid transformation occurs from hcp to fcc and simultaneously the composition drops to about $Pt_{55}Co_{45}$, the same metastable situation encountered for the thin case.

Above 670 K, chemical order appears in the fcc alloy phase, for the films $\geqslant$3 ML. This was observed for the HT alloy as a faint p(2×2) LEED superstructure and as new rods at fractional positions in x-ray diffraction. Anomalous x-ray scattering measurements at the Co K and Pt L_{III} edges were used to determine the structure factor of the superstructure reflections. This order is compatible either with a $L1_2$ structure or with the three domains of the $L1_0$ structure. Segregation was also found systematically when alloying develops, and consistent results were found with LEED, Auger and x-rays. When a quantitative determination of the composition profile could be made, the result was consistent with the systematic trends which we determined earlier at the (111) surface of bulk alloys.

Acknowledgments

Beam time at ESRF is acknowledged on ID3 where preliminary experiments were performed, as well as stimulating discussions with S Ferrer, X Torelles, J Alvarez (ESRF) and J Thiele, C Guillot and L Barbier (CEA, Saclay); and on BM 32, the French CRG-Interface beamline, where all the experiments presented in this paper were performed. We also acknowledge very stimulating discussions with B Legrand (CEA, Saclay) and his PhD student C Gallis (now at Eindhoven University) and with G Tréglia (CNRS-CRMC2, Marseille) on the theoretical aspects of segregation and dissolution in this system. Finally Cray computer time was available from the CNRS IDRIS for the preliminary LEED calculations.

References

[1] See for instance, for theoretical aspects, Christensen A, Ruban A V, Stotze P, Jacobsen K W, Skriver H L, Norskov J K and Besenbacher F 1997 *Phys. Rev.* B **56** 5822
For an experimental study, Murray P W, Stensgaard I, Laegsgaard E and Besenbacher F 1996 *Surf. Sci.* **365** 591

[2] Foiles S M 1990 Calculation of the surface segregation of alloys using the embedded atom method *Segregation and Related Phenomena* ed P Dowben and A Miller (Boca Raton, FL: CRC Press) pp 79–108

[3] Legrand B, Tréglia G and Ducastelle F 1990 *Phys. Rev.* B **41** 4422
Senhadji A, Tréglia G, Eugène J, Khoutami A and Legrand B 1993 *Surf. Sci.* **287** 371
Gallis C, Legrand B, Saul A, Tréglia G, Hecquet P and Salanon B 1996 *Surf. Sci.* **352** 588

[4] Leroux C, Cadeville M C, Pierron-Bohnes V, Inden G and Hinz F 1988 *J. Phys. F: Met. Phys.* **18** 2033–51

[5] Maykov V V, Yermakov A Y, Ivanov G V, Khrabrov V I and Magnat L M 1989 *Phys. Met. Mettal.* **67** 76

[6] Kootte A, Haas C and de Groot R A 1991 *J. Phys.: Condens. Matter* **3** 1133

[7] Weller D, Brändle H and Chappert C 1993 *J. Magn. Magn. Mater.* **121** 461

[8] Beaurepaire E, Maret M, Halté V, Merle J C, Daunois A and Bigot J Y 1998 *Phys. Rev.* B **58** 12–134

[9] Gauthier Y 1996 Pt-metal alloy surfaces: systematic trends *Proc. Int. Workshop on 'Physics and Chemistry of Alloy Surfaces (Dresden, Germany, April 17–20, 1994) Surf. Rev. Lett.* **3** 1663–89 and references therein
Gauthier Y, Dolle P, Baudoing-Savois R, Hebenstreit W, Platzgummer E, Schmid M and Varga P 1998 Chemical ordering and reconstruction of $Pt_{25}Co_{75}(100)$: a LEED/STM study *Surf. Sci.* **396** 137–55

[10] Tréglia G and Legrand B 1995 Private communication
Tréglia G and Legrand B 1997 Private communication
Tréglia G and Legrand B 1998 Private communication

[11] Maret M, Cadeville M C, Staiger W, Beaurepaire E, Poinsot R and Herr A 1996 *Thin Solid Films* **275** 224

[12] de Bersuder L 1974 *Rev. Sci. Instrum.* **45** 1569
Aberdam D, Baudoing R and de Bersuder L 1974 *Rev. Sci. Instrum.* **45** 1573

[13] Baudoing-Savois R *et al* 1999 *Nucl. Instrum. Methods* B **149** 213

[14] French beamline BM32 (CRG-IF), run at the European Synchrotron Radiation Facility, Grenoble, France

[15] Vlieg E, Robinson I K and Kern K 1990 *Surf. Sci.* **233** 248

[16] See for instance the comparable uncertainties obtained for the parallel and normal parameters of atoms in the two outermost layers in a case of chemisorption (Ni(100)-P4g-(2×2)-C, Gauthier Y, Baudoing-Savois R, Heinz K and Landskron K 1991 *Surf. Sci.* **251** 493)
or in a case of reconstruction Pt(110) (1×2), Fery P, Moritz W and Wolf D 1988 *Phys. Rev.* B **38** 7275

[17] Bugnard J M, Gauthier Y and Baudoing-Savois R 1995 *Surf. Sci.* **344** 42–50

[18] Ascolani H, Cerda J R, de Andres P L, de Miguel J J, Miranda R and Heinz K 1996 *Surf. Sci.* **314** 320–30

[19] Bugnard J M 1995 *Thesis* Université Joseph Fourier, Grenoble, France

[20] Dolle P, Gauthier Y and Baudoing-Savois R 1996 *5th Int. Conf. on the Structure of Surfaces (ICSOS) (Aix en Provence, July 9–12, 1996)*

[21] Saint Lager M C, De Santis M, Dolle P, Gauthier Y and Baudoing-Savois R 1996 *Science at ESRF (ESRF Users' Meeting) (Grenoble Nov 1996)*
Saint Lager M C, De Santis M, Dolle P, Gauthier Y and Baudoing-Savois R 1997 *Highlight ESRF 1997*

[22] ESRF reports: preliminary experiment SI 101 (Sept. 95); experiments: 32-3-09 (Mai 96), SI-202 (Dec. 96), 32-3-17 (Avr. 97) Baudoing-Savois R, De Santis M, Dolle P, Gauthier Y and Saint Lager M C 1997 E-MRS June 1997, Strasbourg, France

[23] Ferrer S, Alvarez J, Lundgren E, Torelles X, Fajardo P and Boscherini F 1997 *Phys. Rev.* B **56** 9848

[24] McGee N W E, Johnson M T, de Vries J J and de Stegge J 1993 *J. Appl. Phys.* **73** 3418

[25] Atrei A, Galeotti M, Bardi U, Torrini M, Zanazzi E and Rovida G 1995 *Surf. Rev. Lett.* **2** 279–83

[26] Thiele J, Barrett N T, Belkhou R, Guillot C and Koundi H 1994 *J. Phys.: Condens. Matter* **6** 5025

[27] Grütter P and Dürig U T 1994 *Phys. Rev.* B **49** 2021

[28] Tsay J S and Shern C S 1998 *Surf. Sci.* **396** 313

[29] Thiele J, Belkhou R, Bulou H, Heckmann O, Magnan H, Le Fèvre P, Chandesris D and Guillot C 1997 *Surf. Sci.* **384** 120

[30] Bolzoni F, Leccabue F, Panizzieri R and Perei L 1984 *IEEE Trans. Magn.* **20** 1625

[31] Dahmani C E 1985 *Thèse* Université Louis Pasteur, Strasbourg

[32] Schmid M, Stadler H and Varga P 1993 *Phys. Rev. Lett.* **70** 1441

[33] Gauthier Y, Baudoing-Savois R, Bugnard J M, Bardi U and Atrei A 1992 *Surf. Sci.* **276** 1 (for $Pt_{80}Co_{20}(111)$)
Gauthier Y, Baudoing-Savois R, Rosink H and Sotto M 1993 *Surf. Sci.* **297** 193-201 for $Pt_{25}Co_{75}(111)$
Gauthier Y, Dolle P, Baudoing-Savois R, Hebenstreit W, Platzgummer E, Schmid M and Varga P 1998 *Surf. Sci.* **396** 137 (for $Pt_{25}Co_{75}(100)$)

[34] du Plessis J and Viljoen E C 1996 *Surf. Sci.* **357** 905
[35] Saint-Lager M C, Baudoing-Savois R, De Santis M, Dolle P and Gauthier Y 1998 *Surf. Sci.* **418** 485
[36] Saint-Lager M C, Baudoing-Savois R, De Santis M and Dolle P 1998 États métastables des couches ultra-minces d'alliages Pt–Co. Initiation et propagation de l'ordre 11 *Surface et Interfaces* **11** 25–6
[37] Ristau R A, Barmak K, Coffey K R and Howard J K 1997 *Proc. Symp. on Magnetic Ultrathin Films, Multilayers and Surfaces (San Francisco, 1997)* (Pittsburgh, PA: Material Research Society) p 119
[38] De Santis M, Baudoing-Savois R, Dolle P, Saint-Lager M C and Gauthier Y 1999 Long range order in ultra-thin Pt-Co(111) alloys *Surf. Rev. Lett.* **6** 361–8
[39] Thiele J, Belkhou R, Bulou H, Heckmann O, Magnan H, Le Fèvre P, Chandesris D and Guillot C 1997 *Surf. Sci.* **384** 120